Impact of orbital decay and recoil mergers kicks on the growth of SMBHs

Sebastian Bustamante

Contents

1 Dynamical friction in SMBHs

2 Spin evolution of SMBHs

The angular momentum of a SMBH is defined by the following expression:

$$J_{bh} = |a| \frac{GM_{bh}^2}{c} \tag{1}$$

where a is the spin parameter, satisfying the condition $0 \leq |a| \leq 1$. This is imposed from assuming a rotating Kerr BH, where the maximum spin allowed for a BH is GM_{bh}^2/c.

We assume two main processes through which BHs can be spun up or spun down, namely gas accretion and BH-BH binary coalescence. For gas accretion, we model spin evolution of SMBHs by adopting the model presented by **?**.

2.1 Modelling gas accretion

We assume here that a gas accretion disk is formed around the BH if the mass accretion rate is above 1% of the Eddington rate (**?**). For accretion rates below this value, the gas does not carry enough angular momentum to modify significantly the spin of the BH. Additionally, we assume a thin Shakura-Sunyaev disk model (**?**).

2.1.1 Spin evolution equation

Once the accretion disk is set, the orbiting gas loses its angular momentum due to viscous torques caused by magnetic fields (**?**), moving inwards and reaching then the radius of the last stable orbit (LSO) of the BH, which can be expressed in terms of the BH's spin (**?**):

$$\hat{r}_{lso} = \frac{r_{lso}}{R_g} = 3 + Z_2 \pm [(3 - Z_1)(3 + Z_1 + 2Z_2)]^{1/2} \tag{2}$$

where the negative sign is taken for a counter-rotating BH (i.e. $a < 0$) and positive in case of co-rotation. Also, for convenience, a normalization with the gravitational radius R_g is used, which is defined as half of the Schwarzschild radius:

$$R_g = \frac{R_{Schw}}{2} = \frac{GM_{bh}}{c} \tag{3}$$

finally, the quantities Z_1 and Z_2 depend on the BH's spin, and are defined as:

$$Z_1 \equiv 1 + (1 - a^2)^{1/3} \left[(1 + a)^{1/3} + (1 - a)^{1/3} \right] \tag{4}$$

$$Z_2 \equiv (3a^2 + Z_1^2)^{1/2} \tag{5}$$

Once the gas reaches the edge of the accretion disk at the LSO, we assumed that is immediately accreted, adding up to the total BH's mass and angular momentum:

$$dM_{bh} = \frac{\tilde{e}}{c^2} dM_0, \quad dJ_{bh} = \tilde{l}_{lso} dM_0 \tag{6}$$

where $\tilde{e}$ and $\tilde{l}$ are the energy and angular momentum per unit rest mass of the infalling gas and dM_0 the mass of an accreted gas parcel. The differential equation for the evolution of the spin can be then derived from the previous expressions, yielding:

$$\frac{da}{d \ln M_{bh}} = \frac{1}{M_{bh}} \frac{c^3}{G} \frac{\tilde{l}_{lso}}{\tilde{e}_{lso}} - 2a \tag{7}$$

which can be integrated to obtain the final evolution equation (**?**):

$$a^f = \frac{1}{3} \hat{r}_{lso}^{1/2} \frac{M_{bh}}{M_{bh}^f} \left[1 - \left\{ 3\hat{r}_{lso} \left(\frac{M_{bh}}{M_{bh}^f} \right)^2 - 2 \right\}^{1/2} \right], \quad \frac{M_{bh}^f}{M_{bh}} \leq \hat{r}_{lso}^{1/2} \tag{8}$$

$$a^f = 0.998, \quad \frac{M_{bh}^f}{M_{bh}} > \hat{r}_{lso}^{1/2} \tag{9}$$

where M_{bh}^f and a_{bh}^f are the mass and the spin of the BH after the accretion episode. Bardeen's original formula assigns a maximum spin value of 1 once the final-initial mass ratio is above $\tilde{r}_{lso}^{1/2}$, however, following the argument of **?**, the accretion disk radiates and some of these photons are accreted by the BH. Photons with angular momentum opposite to the spin of the BH will then counteract it, thereby reducing the maximum value that can be reached, setting an upper limit of $a = 0.998$.

2.1.2 Accreting gas in misaligned disks

The previous discussion led us to obtain the formula to calculate spin evolution once a mass $M_b = M_{bh}^f - M_{bh}$ is accreted by the BH. However, we still need to estimate this mass. In order to do so, we assume the most general situation where a tilted and warped accretion disk forms around the BH. We define the angular momentum of the BH and the disk as $\boldsymbol{J}_{bh}$ and $\boldsymbol{J}_d$ respectively. The total angular momentum is defined then as:

$$\boldsymbol{J}_{tot} = \boldsymbol{J}_{bh} + \boldsymbol{J}_d \tag{10}$$

due to conservation of angular momentum in the BH-disk system, this vector is constant (magnitude and orientation) during the whole accretion episode.
In Figure 1 it is defined the relative orientation of the vectors. θ is the angle between the BH and the disk angular momentum and satisfies that $0 \leq \theta \leq \pi$. $\theta = 0$ and $\theta = \pi$ correspond to full alignment and anti-alignment respectively. The angle θ^t is defined as the angle between the BH's spin and the total angular momentum.

Using 10, the angle θ satisfies the next equation:

$$J_{tot}^2 = J_{bh}^2 + J_d^2 = 2J_{bh}J_d \cos\theta$$

or

$$\cos\theta = \frac{J_{tot}^2 - J_{bh}^2 - J_d^2}{2J_{bh}J_d} \tag{11}$$

In the same way, for θ^t:

$$J_{bh}\cos\theta^t + J_d\cos(\theta - \theta^t) = J_{tot}$$

$$J_{bh}\sin\theta^t = J_d\sin(\theta - \theta^t) \tag{12}$$

Figure 1: Warped accretion disk around a SMBH. Figure taken from **?** (Fig 2).

Due to the torque caused by the Lense-Thirring effect, the gas around the disk in a misaligned system will precess around the rotation axis of the BH, and if strong viscosity gradients are present, an inner part of the disk will be forced to lay in the equatorial plane of the BH, causing thus an inner warped region in the disk (**?** and references within). The precession rate is given by (**?**):

$$\mathbf{\Omega}_p = \frac{2G\mathbf{J}_{bh}}{c^2R^3}$$

4

From this, the following timescales are defined: the precession timescale $t_{prec}(R)$, viscous accretion timescale $t_{\nu_1}(R)$ and warp propagation timescale $t_{\nu_2}(R)$ and , which are defined respectively as:

$$t_{prec}(R) \equiv \frac{2\pi}{\Omega_p(R)} \tag{13}$$

$$t_{\nu_1}(R) \equiv \frac{R^2}{\nu_1(R)} \tag{14}$$

$$t_{\nu_2}(R) \equiv \frac{R^2}{\nu_2(R)} \tag{15}$$

Where ν_1 and ν_2 are the kinematic viscosities acting on velocity gradients parallel and perpendicular to the plane of the disk respectively. Following ?, we adopt $\nu_2 = \nu_1/\alpha^2$ and the Shakura-Sunyaev parameter $\alpha = 0.1$.

In order to estimate the radius of the warped region R_{warp}, the timescales for precession and warp propagation are compared, such that

$$t_{prec}(R_{warp}) = t_{\nu_2}(R_{warp})$$

Inside the warp region, we have the condition $t_{prec} \leq t_{\nu_2}$, which means that precession is fast enough to avoid viscosity effects propagated in the normal direction to the plane, thereby keeping the inner region warped. Outside this region, viscosity effects can counteract the deformation. In terms of the Schwarzschild radius, the warp radius is given by (?):

$$\frac{R_{warp}}{R_{Schw}} = 3.6 \times 10^3 a^{5/8} \left(\frac{M_{bh}}{10^8 M_\odot} \right)^{1/8} \lambda^{-1/4} \left(\frac{\nu_2}{\nu_1} \right)^{-5/8} \alpha^{-1/2} \tag{16}$$

where $\lambda \equiv L/L_{Edd}$ is the Eddington ratio.

To estimate the mass accreted by the BH, we assume that the whole mass inside the warp region is accreted in the accretion timescale t_{ν_1}, obtaining:

$$M_d(R_{warp}) = \dot{M} t_{\nu_1}(R_{warp}) \tag{17}$$

where $\dot{M}$ is the mass accretion rate of the BH. Using equation 16, the accretion timescale at the edge of the warp region is:

$$t_{\nu_1} = \frac{R_{warp}^2}{\nu_1} = 3 \times 10^6 a^{7/8} \left(\frac{M_{bh}}{10^8 M_\odot} \right)^{11/8} \lambda^{-3/4} \left(\frac{\nu_2}{\nu_1} \right)^{-7/8} \alpha^{-3/2} \ yr \tag{18}$$

Finally, we used the alignment condition proposed by ? to evaluate whether the BH is aligned or counter-aligned to the accretion disk:

$$\cos\theta < -\frac{J_d}{2 J_{bh}} \tag{19}$$

Using the expressions for the Schwarzschild and warp radius, we obtain

$$\frac{J_d}{2J_{bh}} = 10^{-9}\lambda \left(\frac{t_{\nu_1}}{1\ yr}\right)\left(\frac{R_{warp}}{R_{Schw}}\right)^{1/2} a^{-1}$$

2.1.3 Numerical implementation

The previous formulation of disk accretion by **?** was based on semi-analytical models of galaxy formation, where halos are tracked in the Millenium N-body simulation. Therefore, the accretion rate and the total mass budget to feed a BH were estimated semi-analytically from merger histories. Here instead, we couple in a self-consistent way the spin evolution and the numerical outputs for the accretion rate and accreted mass in the AREPO code. The following steps are followed in the code:

1. In cosmological setups, when a fof halo reaches a threshold mass M_{th}, a BH is seeded in the potential minimum. We initialize the spin of the BH with an initial value $a_{bh,0}$ in a random direction. For non-cosmological setups, in the first time-step, the spin of every BH is also initialize in the same way. We adopt a conservative value of $a_{bh,0} = 0$, however we will explore different choices.

2. Using the BH mass M_{bh}, we proceed to calculate the quantities R_{warp}, $M_d(R_{warp})$ and the angular momentum of the disk $J_d(R_{warp})$.

3. A normal vector is drawn for the plane of the accretion disk. This can be done either by randomly draw a vector or by using a parallel vector to the angular momentum of the gas cells used to compute the local density around the BH. This way, we get the initial angles θ and θ^t. The total angular momentum $\boldsymbol{J}_{tot}$ is also computed in this step, and is kept constant during the whole accretion episode.

3 Recoil merger kicks

3.1 Modelling recoils

In order to model gravitational recoils of BHs, we used the same approach followed by Sijacki et al. (2009). Three different cases of recoils are studied, namely mass asymmetry driven recoils, recoils in configurations with arbitrary mass and aligned/anti-aligned spins, and finally, configurations with arbitrary mass and arbitrary spin orientation. The last case is the most general one and will be the approach implemented in the code[1]. In the following part, the three different approaches are covered in detail.

---

[1]This also means that spin evolution has to be followed in the code. It is necessary to learn how to add new properties to a particle type in AREPO.

3.1.1 Mass asymmetry driven recoils

In this case, the recoil is purely driven by the mass asymmetry of the two involved BHs. We follow the Fitchett formula numerically calibrated by González et al. (2007):

$$v_{\text{m, kick}} = A\eta^2 \sqrt{1 - 4\eta}(1 + B\eta) \tag{20}$$

where the parameters A and B are 1.2×10^4 km/s and -0.93 respectively, and the parameter η is defined as $\eta = q/(1 + q)^2$, with $q = m_1/m_2 \leq 1$.

Although the two involved BHs have a null spin, the remnant will acquire a non-zero value due to the angular momentum carried away by the gravitational waves (GW). The formula for the spin gained by the remnant is given by:

$$a_{\text{fin}} = 3.464\eta - 2.029\eta^2 \tag{21}$$

3.1.2 Configuration with arbitrary mass ratio and aligned/anti-aligned spins

In this second case, both BHs are allowed to have a spin in the direction of the orbital angular momentum of the binary system, either aligned or anti-aligned. In this case, the recoil velocity can reach higher values (up to 460 km/s). The standard formula is given by:

$$\vec{v}_{\text{align, kick}} = v_{\text{m, kick}}\hat{e}_1 + v_\perp(\cos\xi\hat{e}_1 + \sin\xi\hat{e}_2) \tag{22}$$

with

$$v_\perp = H\frac{\eta^2}{1 + q}(a_2 - qa_1) \tag{23}$$

Here, $\hat{e}_1$ and $\hat{e}_2$ are orthogonal vectors lying in the orbital plane. ξ is an angle between the unequal mass and spin contribution to kick velocity. Here, it is adopted the value $\xi = 90^o$. For the parameter H, we adopt the same value as in Campanelli et al. (2007), i.e. $H = 7.3 \times 10^3$ km/s.

3.1.3 Configuration with arbitrary mass ratio and random spin orientation

For this last case, both BHs are allowed to have an arbitrary mass and a random spin orientation. The recoil velocity is then given by the next formula:

$$\vec{v}_{\text{align, kick}} = v_{\text{m, kick}}\hat{e}_1 + v_\perp(\cos\xi\hat{e}_1 + \sin\xi\hat{e}_2) + v_\parallel\hat{e}_z \tag{24}$$

where

$$v_\parallel = K\cos(\Theta - \Theta_0)\frac{\eta^2}{1 + q}(a_2^\perp - qa_1^\perp) \tag{25}$$

Here, $K = 6 \times 10^4$ km/s, $\Theta_0 = 0.184$. Θ is defined as the angle between the in-plane component of the vector $\vec{\Delta} = (m_1 + m_2)(\vec{a_1} - \vec{a_2})$ and the infall direction at the merger,

which is taken as the radial direction just before the coalescence. In figure 2 we show the reference system used to apply the recoil velocity to the remnant.
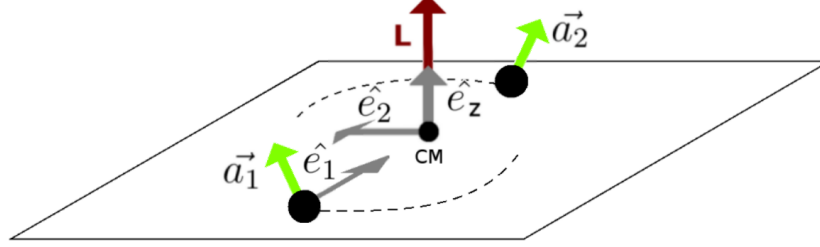

Figure 2: Reference system that is used to apply the recoil velocity of the BH remnant.

We also correct for the eccentricity of the orbit using the formula proposed by (Sopuerta et al., 2007):

$$\vec{v}_e = \vec{v}_{\text{align, kick}} (1 + e) \tag{26}$$

This approach is the most general one and will be implemented in our study.

3.2 Numerical implementation

In order to adapt the previous scheme to our simulations, we adopt a series of assumptions that facilitates the numerical implementation, namely:

- Only merger events involving two BHs take place in the simulation. Three-BHs merger events are split up in two two-BHs mergers.

- The two BHs will merge once they are closer than the minimum of the softening lengths used to compute the gas density for each BH.

- They will merge irrespectevely of their approach velocity. Usually, a criterion based on the local speed of sound would provide a more realistic scenario, however, as a first-order estimative, we do not apply this.

- The reference system used in the estimation of the kick velocity is built based on the state of the system just before the numerical coalescence. This clearly differs from the physical coalescence as the binary system should take some time before the merger event, which happens after the distance becomes less than smoothing length. However, this scale is by no means, well-resolved in our simulations, so we neglect this time. We also assume that the angular momentum is not significantly changed during the coalescence phase and the orbital plane, which defines our recoil system, can be taken as the same in the numerical coalescence.

8

- Spin evolution is not considered here (at the moment). We assume that BHs accrete mass in a chaotic and episodic way, as proposed by King et al. (2008). This accretion mode regularize the spin of the BH as the infalling matter does not contribute constructively to spin up the BH. The random and chaotic nature of the accretion makes the spin quickly converge to a value of $a = 0.3 \pm 0.2$.

3.2.1 Setting up the spins

Merger events are the only processes that can significantly spin up a BH, however the spin of the remnant should be quickly slowed down by chaotic and episodic gas accretion in a presumably short time scale, thereby erasing any "memory" of the initial conditions or the last merger (King et al., 2008). Instead of following spin evolution, we set up a random oriented spin for each BH prior to a merger. The magnitude of the spin parameter is generated based on a normal distribution with $\bar{a} = 0.3$ and $2\sigma = 0.2$.
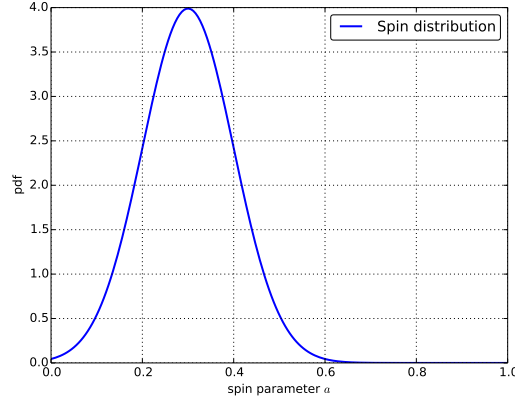

Figure 3: Spin distribution function to generate initial values prior to a merger.

3.2.2 Defining reference system

Prior to the merger, we have the next information from the two involved BHs: m_1, $\vec{r_1}$, $\vec{v_1}$, m_2, $\vec{r_2}$, $\vec{v_2}$ along with the two randomly generated spins $\vec{a_1}$ and $\vec{a_2}$. From this information, we proceed to construct the reference system where the recoil merger kick will be referred. The respective two-body variables are then $\vec{r} = \vec{r_1} - \vec{r_2}$ and $\vec{v} = \vec{v_1} - \vec{v_2}$. The angular momentum of the binary is $\vec{L} = \vec{r} \times \vec{v}$. We define the orthonormal system $\hat{e}_1$, $\hat{e}_2$, $\hat{e}_z$ as $\hat{e}_1 = \vec{r}/r$, $\hat{e}_z = \vec{L}/L$ and $\hat{e}_2 = \hat{e}_z \times \hat{e}_1$

References

Campanelli M., Lousto C., Zlochower Y., Merritt D., 2007, ApJL, 659, L5

González J. A., Hannam M., Sperhake U., Brügmann B., Husa S., 2007, Physical Review Letters, 98, 231101

King A. R., Pringle J. E., Hofmann J. A., 2008, MNRAS, 385, 1621

Sijacki D., Springel V., Haehnelt M. G., 2009, MNRAS, 400, 100

Sopuerta C. F., Yunes N., Laguna P., 2007, ApJL, 656, L9